

A Search for Vector Diquarks at the CERN LHC

E. Arıka^a, O. Çakır^b, S.A. Çetin^a and S. Sultansoy^{c,d}

^a Bogazici University, Faculty of Sciences, Department of Physics,
80815, Bebek, Istanbul, Turkey

^b Ankara University, Faculty of Sciences, Department of Physics,
06100 Tandoğan, Ankara, Turkey

^c Gazi University, Faculty of Arts and Sciences, Department of Physics,
06500, Teknikokullar, Ankara, Turkey

^d Azerbaijan Academy of Sciences, Institute of Physics,
H. Cavid av., 33, Baku, Azerbaijan

Resonant production of the first generation vector diquarks at the CERN Large Hadron Collider (LHC) have been investigated. It is shown that the LHC will be able to discover vector diquarks with masses up to 9 (8) TeV if coupling $D^{\prime\prime} \rightarrow s(\bar{s})$.

I. INTRODUCTION

The existence of at least three fermion families naturally leads to the hypothesis that they are made up of more fundamental constituents frequently called preons [1]. Today, the compositeness should be considered as a candidate for beyond the standard model (BSM) physics on the same footing as SUSY. Moreover, some assumptions made in order to get rid of huge number of free parameters in three family MSSM have natural explanation (see [2] and references therein) in the framework of preonic models. These models predict a rich spectrum of new particles with unusual quantum numbers at high energies such as excited quarks and leptons, diquarks, dileptons, leptoquarks, leptogluons, sextet quarks, octet bosons etc. In preonic models, diquarks are as natural as leptoquarks [3]. They are colored objects having integer-spin and baryon number $B_J = 2=3$. Diquarks are also predicted in the framework of superstring-inspired E_6 models [4].

Recent collider limits on the diquark masses come from Tevatron data which exclude the region $290 < M < 420$ GeV (for E_6 diquarks) [5]. Diquark production at e^+e^- colliders, ep colliders and pp colliders have been analyzed in [6], [7] and [8], respectively. Recently, the resonance production of scalar diquarks at CERN LHC has been studied in [9].

In this work, the sensitivity of LHC to composite vector diquark production is estimated. In section II, interaction lagrangian and quantum numbers of diquarks are discussed. Decay width and production cross section of a vector diquark at the CERN LHC are considered in section III. Then, in section IV, vector diquark signal and corresponding backgrounds are analyzed. Finally, in section V we give some conclusions and remarks.

II. INTERACTION LAGRANGIAN AND CLASSIFICATION

A model independent, most general, effective $SU(3)_C \times SU(2)_W \times U(1)_Y$ invariant lagrangian for diquarks has the form [9]:

$$\begin{aligned} L = & g_{1L} q_L^c i_2 q_L^c D_1^c + g_{1R} u_R^c d_R^c D_1^c + g_{1R} d_R^c d_R^c D_1^c + g_{1R}^0 u_R^c u_R^c D_1^0 + g_{3L} q_L^c i_2 \sim q_L^c D_3^c \\ & + g_2 D_2^{CT} d_R^c i_2 \sim q_L^c + g_2 D_2^{CT} u_R^c i_2 \sim q_L^c + h.c. \end{aligned} \quad (1)$$

where $q_L^c = (u_L; d_L)$ and $q^c = C q^T$ ($q^c = q^T C^{-1}$). For the sake of simplicity, color and generation indices are omitted. Scalar diquarks D_1, D_1^0, D_3 are $SU(2)_W$ singlets and D_3 is $SU(2)_W$ triplet. Vector diquarks D_2 and D_2^0 are $SU(2)_W$ doublets. Diquarks may transform as antitriplet or sextet under $SU(3)_C$. At this stage, we assume each SM generation has its own diquarks and couplings in order to avoid restrictions imposed by m_K etc.

Lagrangian (1) can be rewritten in the following more transparent form:

$$L = L_S + L_V \quad (2)$$

$$\begin{aligned} L_S &= g_{1L} u^c P_L d - d^c P_L u + g_{1R} u^c P_R d - D_1 + g_{1R} d^c P_R d D_1 + g_{1R}^0 u^c P_R u D_1^0 \\ &+ p \bar{2} g_{3L} u^c P_L u D_3 + p \bar{2} g_{3L} d^c P_L d D_3 - g_{3L} u^c P_L d + d^c P_L u D_3^0 + h.c. \end{aligned} \quad (3)$$

$$L_V = g_2 d^c P_L d D_2^1 - g_2 d^c P_L u D_2^2 + g_2 u^c P_L d D_2^1 - g_2 u^c P_L u D_2^2 + h.c. \quad (4)$$

where $P_L = (1 \quad 5) = 2$ and $P_R = (1 \quad 5) = 2$. A general classification of the first generation, color 3 diquarks is shown in Table I.

III. DECAY WIDTH AND PRODUCTION CROSS SECTION

For the present analysis, we will take into account the color 3 vector diquark D_2 which couples to ud -pair as described by the effective lagrangian (4). The decay width Γ_D , derived from the same lagrangian, is

$$\Gamma_D = C_F \frac{g_2^2 M_D}{24} \quad (5)$$

where C_F is the color factor for triplet representation and M_D is the mass of vector diquark. We will use the definition $g_2^2 = 4 \Gamma_D$ for numerical calculations:

$$\Gamma_D = C_F \frac{D M_D}{6} \cdot 17 \text{ GeV} \left(\frac{C_F M_D}{1 \text{ TeV}} \right) \text{ for } D = 0.1 \cdot s \quad (6)$$

$$\cdot 13 \text{ GeV} \left(\frac{C_F M_D}{1 \text{ TeV}} \right) \text{ for } D = s_{em} : \quad (7)$$

In the narrow width approximation ($M_D \ll 0.1$), the cross section of the s-channel diquark resonance production can be obtained as

$$(pp \rightarrow D_2 X) = \frac{X}{ab} \frac{C_F^2 D^2}{s} \int_{M_D^2/s}^{Z_1} \frac{dx}{x} f_a(x; \hat{s}) f_b \left(\frac{M_D^2}{sx}; \hat{s} \right) \quad (8)$$

where $\hat{s} = x_a x_b s$, f_a and f_b are quark distribution functions of each proton. In Fig. 1, using the CTEQ 5L quark distribution functions [10], the cross section versus diquark mass is plotted for coupling $D = s$ and $D = s_{em}$ at the LHC energy ($\sqrt{s} = 14 \text{ TeV}$).

IV. SIGNAL AND BACKGROUND

D_2 -type diquark resonance in s-channel will be formed via the subprocess $u + d \rightarrow D_2 + u + d$. Therefore, the signal will contain two hard jets in the final state. Considering only the interference with the t-channel gluon exchange, the following differential cross section is obtained:

$$\begin{aligned} \frac{d\hat{\sigma}}{d\hat{t}} (q_i q_j \rightarrow q_k q_l) &= C_F^2 \left[\frac{\frac{2}{D} (\hat{s} + \hat{t})^2}{\hat{s}^2 [(\hat{s} - M_D^2)^2 + M_D^2]} \right. \\ &\left. + \frac{2 \frac{2}{s}}{\hat{s}^2} \frac{(2\hat{s}^2 + \hat{t}^2 + 2\hat{s}\hat{t})}{\hat{t}^2} - \frac{2 \frac{2}{D} s}{\hat{t}^2} \frac{(\hat{s} + \hat{t})^2 (\hat{s} - M_D^2)}{\hat{s}^2 [(\hat{s} - M_D^2)^2 + M_D^2]} \right] : \quad (9) \end{aligned}$$

At the LHC, QCD processes contributing to two jet final states and their integrated cross sections are given in Table II. The values in Table II have been generated by PYTHIA 6.1 [11] at parton level with various p_T cuts.

The cross section as a function of the dijet invariant mass M_{jj} with the rapidity cut $|y_{1,2}| \leq Y$, where y_1 and y_2 are rapidities of the massless final quarks, is given by

$$\frac{d}{dM_{jj}} = \frac{M_{jj}^3}{2s} \int_0^{\infty} dy_2 \int_{y_1^{\text{min}}}^{y_1^{\text{max}}} dy_1 \frac{1}{\cosh^2 y^2} [f_{u=A}(x_u; Q^2) f_{d=B}(x_d; Q^2) \frac{d\hat{s}}{d\hat{t}}(s; \hat{t}; \hat{u}) + f_{d=A}(x_d; Q^2) f_{u=B}(x_u; Q^2) \frac{d\hat{s}}{d\hat{t}}(s; \hat{u}; \hat{t})] \quad (10)$$

with

$$y^2 = (y_1 - y_2)^2 = 2; \quad y^b = (y_1 + y_2)^2 = 2 \\ x_u = p - e^{y^b}; \quad x_d = p - e^{y^b} \\ s = x_u x_d s; \quad \hat{t} = x_u p_T \frac{p}{s} e^{-y_1}; \quad \hat{u} = x_d p_T \frac{p}{s} e^{y_1} \\ y_1^{\text{min}} = \min(\log y_1, \log y_2); \quad y_1^{\text{max}} = \max(\log y_1, \log y_2); \quad M_{jj}^2 = s \quad :$$

Fig. 2 shows jet-jet invariant mass distribution for the process $p\bar{p} \rightarrow D_2 \rightarrow jjX$ together with the estimation of the QCD background at the LHC. For comparison, signal peaks for vector diquark masses $M_D = 2, 4, 6, 8$ TeV and $\beta_D = 0.1$ are superimposed on the background distribution.

We have estimated signal and background events for an integrated LHC luminosity of 10^5 pb^{-1} taking into account, as an example, the energy resolution of ATLAS hadronic calorimeter [12]:

$$\frac{E}{E} = \frac{50\%}{p_T/E} + 3\% \quad (11)$$

for jets with $|y| < 3$. The mass resolution can be expressed as [9]

$$\frac{M_{jj}}{M_{jj}} = \frac{p_T}{2E} \quad : \quad (12)$$

We have chosen $2 M_{jj}$ as the mass window centered at M_{jj} for signal and background estimations.

Number of signal (S), background (B) events and the corresponding significances for $\beta_D = 0.1$ are tabulated in Table III. Evidently, tighter cut on the rapidity y improves the significance considerably. In Table IV, we present the achievable mass limits for different values of β_D . As discovery criteria, we adopt $S/B = 5$ and $S = 25$.

V. CONCLUSIONS

The example of D_2 shows that the resonance production of vector diquarks at the LHC has large cross section. With reasonable cuts, it may be possible to cover the region up to 9 TeV. The LHC potential for the discovery of D_2 is clearly demonstrated in Fig. 3 where minimum integrated luminosities, needed to satisfy the adopted criteria, are plotted as a function of M_D for various β_D values.

V I. REFERENCES

- [1] H . Terazawa, Phys. Rev. 22 (1980) 184; H . Harari, Phys. Rep. 104 (1984) 159; D 'Souza and K alman, P reons, W orld S cientific Publishing, (1992).
- [2] S . Sultansoy, hep-ph/0003269 (2000).
- [3] J.W udka, Phys. Lett. B 167 (1986) 337.
- [4] J.L. Hewett and T.G . Rizzo, Phys. Rep. 183 (1989) 193.
- [5] F . Abe et al., CDF Collaboration, Phys. Rev. Lett. 77 (1996) 5336; B . Abbott et al., D 0 Collaboration, Phys. Rev.. Lett. 80 (1998) 666.
- [6] D . Schaile and P M . Zerwas: Proceedings of the W orkshop on Physics at Future Accelerators, CERN Yellow Report 87-07, Vol. II, p.251 (1987).
- [7] T G . Rizzo, Z . Phys. C 43 (1989) 223.
- [8] V D . Angelopoulos et al., Nucl. Phys. B 292, 59 (1987).
- [9] S . A tag, O . Cak r, and S . Sultansoy, Phys. Rev. D 59, 015008 (1998).
- [10] CTEQ Collaboration, H L. Lai et al., Eur. Phys. J. C 12 (2000) 375.
- [11] Torbjörn Sjöstrand et al., hep-ph/0010017 (2000).
- [12] ATLAS Collaboration, ATLAS TDR 14, CERN /LHCC 99-14 (1999).

TABLE I. Quantum numbers of the first generation, color 3 diquarks described by the effective lagrangian given in the text according to $SU(3)_C \times SU(2)_W \times U(1)_Y$ invariance. $Q_{em} = I_3 + Y = 2$

| Scalar Diquarks | $SU(3)_C$ | $SU(2)_W$ | $U(1)_Y$ | Q | Couplings |
|-----------------|-----------|-----------|----------|--------|---------------------------------------|
| D_1 | 3^2 | 1 | $2/3$ | $1/3$ | $u_L d_L (g_{1L}) ; u_R d_R (g_{1R})$ |
| D'_1 | 3^2 | 1 | $-4/3$ | $4/3$ | $d_R d_R (g_{1R})$ |
| D_1^0 | 3^2 | 1 | $8/3$ | $-2/3$ | $u_R u_R (g_{1R}^0)$ |
| | | | | $4=3$ | $u_L u_L (\frac{g_{3L}}{2})$ |
| D_3 | 3^2 | 3 | $2/3$ | $1=3$ | $u_L d_L (g_{3L})$ |
| | | | | $2=3$ | $d_L d_L (\frac{g_{3L}}{2})$ |
| Vector Diquarks | | | | | |
| D_2 | 3^2 | 2 | $-1/3$ | $4=3$ | $d_R d_L (g_2)$ |
| | | | | $1=3$ | $d_R u_L (g_2)$ |
| D'_2 | 3^2 | 2 | $5/3$ | $4=3$ | $u_R d_L (g_2)$ |
| | | | | $1=3$ | $u_R u_L (g_2)$ |

TABLE II. Cross sections (pb) for QCD backgrounds contributing to $j\bar{j}$ final states at parton level generated by PYTHIA 6.1 with various cuts.

| Process | $p_T > 100 \text{ GeV}$ | $p_T > 500 \text{ GeV}$ | $p_T > 1000 \text{ GeV}$ | $p_T > 1500 \text{ GeV}$ | $p_T > 2000 \text{ GeV}$ |
|---|-------------------------|-------------------------|--------------------------|--------------------------|--------------------------|
| $gg \rightarrow gg$ | $6.3 \cdot 10^5$ | $2.0 \cdot 10^2$ | $2.3 \cdot 10^0$ | $8.6 \cdot 10^{-2}$ | $5.7 \cdot 10^{-3}$ |
| $q\bar{q} \rightarrow q\bar{q}$ | $6.4 \cdot 10^5$ | $4.8 \cdot 10^2$ | $1.0 \cdot 10^1$ | $6.4 \cdot 10^{-1}$ | $5.7 \cdot 10^{-2}$ |
| $q_i \bar{q}_j \rightarrow q_i \bar{q}_j$ | $1.0 \cdot 10^5$ | $1.8 \cdot 10^2$ | $6.7 \cdot 10^0$ | $6.3 \cdot 10^{-1}$ | $8.8 \cdot 10^{-2}$ |
| $gg \rightarrow q_i \bar{q}_k$ | $2.4 \cdot 10^4$ | $9.8 \cdot 10^0$ | $1.0 \cdot 10^{-1}$ | $4.9 \cdot 10^{-3}$ | $2.9 \cdot 10^{-4}$ |
| $q_i \bar{q}_i \rightarrow q_i \bar{q}_k$ | $1.6 \cdot 10^3$ | $2.8 \cdot 10^0$ | $1.3 \cdot 10^{-1}$ | $9.0 \cdot 10^{-3}$ | $1.1 \cdot 10^{-3}$ |
| $q_i \bar{q}_i \rightarrow gg$ | $1.5 \cdot 10^3$ | $2.5 \cdot 10^0$ | $6.7 \cdot 10^{-2}$ | $8.1 \cdot 10^{-3}$ | $8.5 \cdot 10^{-4}$ |
| Total | $1.4 \cdot 10^6$ | $8.8 \cdot 10^2$ | $1.9 \cdot 10^1$ | $1.4 \cdot 10^0$ | $1.5 \cdot 10^{-1}$ |

TABLE III. Observability of the vector diquark D_2 with $\epsilon_D = 0.1$ at LHC for $L_{int} = 10^5 \text{ pb}^{-1}$.

| $M_D \text{ (TeV)}$ | 1 | 2 | 3 | 4 | 5 | 6 | 7 | 8 | 9 |
|---------------------|------------------|------------------|------------------|------------------|------------------|------------------|------------------|------------------|---------------------|
| $ y < 2$ | | | | | | | | | |
| S | $7.7 \cdot 10^7$ | $6.6 \cdot 10^6$ | $1.1 \cdot 10^6$ | $2.4 \cdot 10^5$ | $5.0 \cdot 10^4$ | $9.9 \cdot 10^3$ | $1.7 \cdot 10^3$ | $2.5 \cdot 10^2$ | $2.7 \cdot 10^1$ |
| B | $2.8 \cdot 10^8$ | $5.6 \cdot 10^6$ | $4.2 \cdot 10^5$ | $5.4 \cdot 10^4$ | $8.4 \cdot 10^3$ | $1.4 \cdot 10^3$ | $2.2 \cdot 10^2$ | $3.0 \cdot 10^1$ | $3.1 \cdot 10^0$ |
| S/B | 4585 | 2787 | 1768 | 1027 | 545 | 266 | 118 | 46 | 16 |
| $ y < 1$ | | | | | | | | | |
| S | $2.6 \cdot 10^7$ | $2.8 \cdot 10^6$ | $5.8 \cdot 10^5$ | $1.3 \cdot 10^5$ | $2.9 \cdot 10^4$ | $6.1 \cdot 10^3$ | $1.1 \cdot 10^3$ | $1.6 \cdot 10^2$ | $1.8 \cdot 10^1$ |
| B | $2.5 \cdot 10^7$ | $5.2 \cdot 10^5$ | $4.0 \cdot 10^4$ | $5.0 \cdot 10^3$ | $7.9 \cdot 10^2$ | $1.3 \cdot 10^2$ | $2.1 \cdot 10^1$ | $2.8 \cdot 10^0$ | $3.0 \cdot 10^{-1}$ |
| S/B | 5213 | 3946 | 2889 | 1842 | 1044 | 534 | 245 | 99 | 34 |

TABLE IV. Achievable diquark mass limits for different diquark-quark-quark couplings in the framework of discovery criteria given in the text. The rapidity cut $|y| < 2$ is applied.

| ϵ_D | $M_D \text{ (TeV)}$ | S | B | S/B |
|--------------|---------------------|------|--------|-------|
| 0.1 | 9 | 27 | 3.1 | 16.0 |
| 0.01 | 8 | 25 | 30 | 4.6 |
| 0.001 | 5 | 500 | 8400 | 5.4 |
| 0.0005 | 4 | 1200 | 540006 | 5.1 |

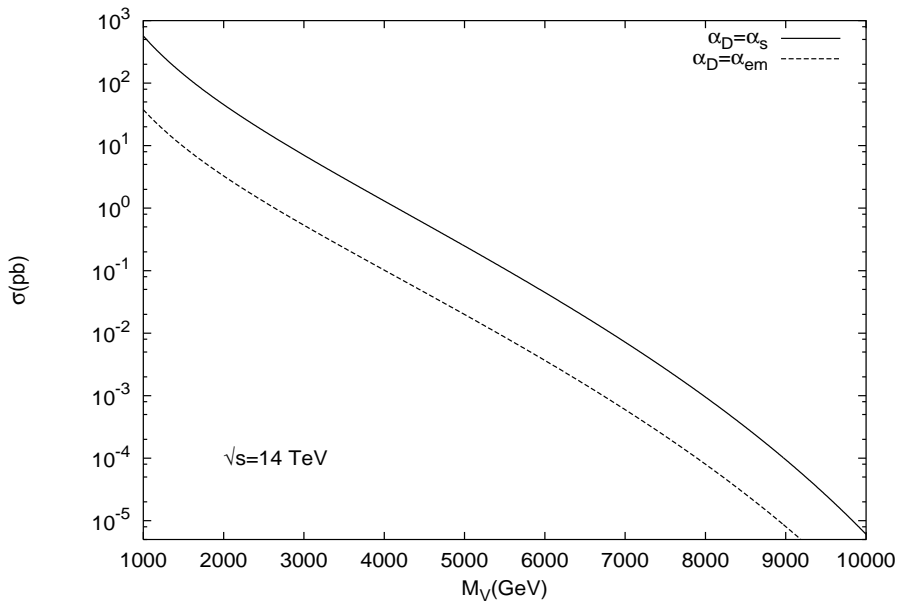


FIG . 1. Integrated cross section versus diquark mass for coupling strength $\alpha_D = \alpha_s$ and $\alpha_D = \alpha_{em}$.

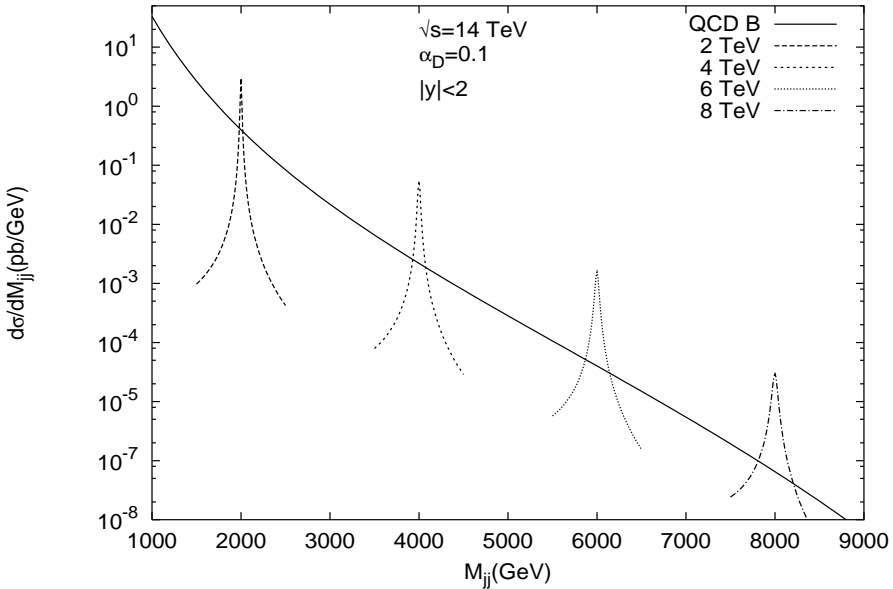


FIG . 2. Dijet invariant mass distribution for $M_D = 2; 4; 6; 8$ TeV superimposed over the QCD background.

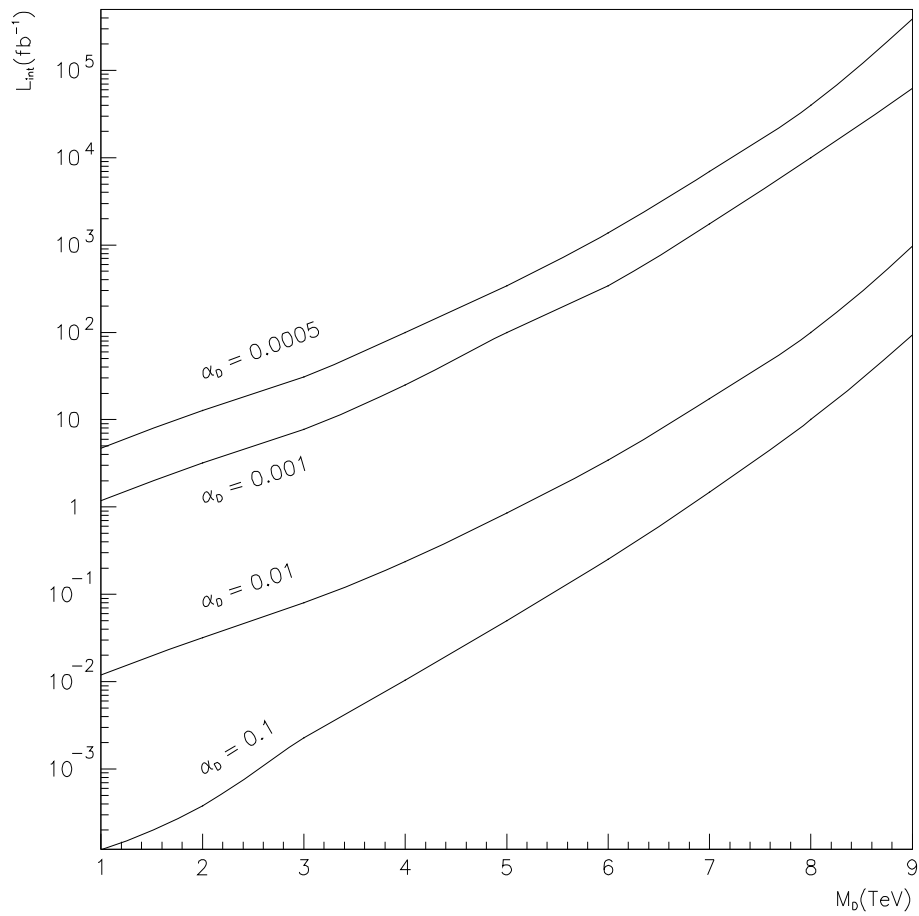


FIG .3. The m inimum integrated lum inosities, needed to satisfy the adopted discovery criteria, as a function of M_{D_0} for various α_0 values.